J. Cent. South Univ. (2014) 21: 3456−3462
DOI: 10.1007/s11771-014-2322-8

Springer

Phase, magnetism and thermal conductivity of glass ceramics from iron ore tailings

CHEN Hao(陈浩)[1], WU Yi-wen(吴益文)[2], ZHANG Hong(张鸿)[1], LI Zhi-cheng(李志成)[1, 3]

1. School of Materials Science and Engineering, Central South University, Changsha 410083, China;
2. Inspection Center of Industrial Products and Raw Materials,
Shanghai Entry-Exit Inspection and Quarantine Bureau of China, Shanghai 200135, China;
3. State Key Laboratory of Powder Metallurgy (Central South University), Changsha 410083, China

Abstract: In order to develop the applications of ore tailings, the glass ceramics were prepared by using a conventional melting-quenching-sintering process. The phase component, microstructures, magnetic properties and thermal conductivities of the prepared glass ceramics were investigated by using X-ray diffractometer, scanning electron microscopy, vibrating sample magnetometer and thermophysical properties tester, respectively. The results show that orthorhombic olivine-type phase and triclinic sunstone-type phase formed when the glass was annealed at 700 ºC, the concentration of olivine-type and sunstone-type phases decreased, the spinel-type cubic phase occurred and the amount increased when the annealing temperatures increased. The magnetic properties from the cubic spinel ferrites were detected in the glass ceramics, and the related saturation magnetization increased with the annealing temperature increasing. The porous glass ceramics with magnetic property showed much lower thermal conductivity, compared with the non-magnetic porous glass-ceramic and the dense glass-ceramics.

Key words: iron ore tailing; glass ceramics; microstructure; magnetic properties; thermal conductivity

1 Introduction

More and more mining tailings were discarded with the developing of mining industries around the world. According to preliminary statistics, the amount of mining tailings in China is more than 10^{12} kg at present. Among various tailings, the amount of iron tailings should be the largest one. It is well known that the mining tailings have brought the serious environment problems [1]. For examples, the vast accumulation of tailings occupies a huge amount of land, and more seriously, the heavy metals (toxic elements) condensed inside the tailings may immerse into groundwater and even enter the rivers, resulting in serious environmental safety. For example, in the accident caused by iron ore tailings dam-break, 276 people died on September 8th 2008 in Xiangfen of Shanxi Province in China. It must be an interesting and important work to develop the applications of various tailings and to reduce the tailing amount. Fortunately, much attention have been recently attracted to develop the multipurpose utilization of iron tailings such as the raw materials for cement production glass, soil fertilizer, filler of dumped mine and purifying industrial chemicals [2−6].

As one kind of polycrystalline solid materials prepared with a basic glass by controlled crystallization, glass ceramics have good physical and chemical properties such as high mechanical property and chemical stability. The glass ceramics have many potential applications in architectural decoration materials, chemical industries, arts and crafts manufacturers, and so on. In recent years, some kinds of industry wastes have been attracted much attention and were used to prepare glass ceramics [7−10]. Various mining tailings have been adopted in the studies of glass ceramics [11−15]. However, most of the previous works aimed at the microstructures and preparation technologies of the glass ceramics, there is few work on the phase transition and microstructure evolution during heat treatment.

The analyses of the evolution of phase component and microstructures of the glass-ceramics made from an iron ore tailing during the heat-treatment process were reported. Magnetic properties and thermal conductivities of the prepared glass-ceramics were also investigated in this work. Owing to the scattering effect of magnetic dipole for electromagnetic wave [16], the magnetic

Foundation item: Project(51172287) supported by the National Natural Science Foundation of China; Project(2012-2013) supported by the Laboratory Research Fund of the State Key Laboratory of Powder Metallurgy, China
Received date: 2013−05−20; **Accepted date:** 2013−10−20
Corresponding author: LI Zhi-cheng, Professor, PhD; Tel: +86−731−88877740; E-mail: zhchli@csu.edu.cn

glass-ceramics should have broad prospects for the applications such as absorbing of electromagnetic wave, thermal insulation and heat preservation.

2 Experimental

The iron ore tailing used in this work was received from an iron mining filed in Inner Mongolia, China. The chemical compositions of iron ore tailing are 43.89% SiO_2, 15.06% Al_2O_3, 10.83% CaO, 10.56% MgO, 14.74% Fe-oxides, 1.38% K_2O, 2.25% Na_2O and 1.14% TiO_2 (mass fraction). In present work, 1.5% of Co_2O_3, NiO and MnO_2, 4.5% of P_2O_5 and 8% of Na_2CO_3 were added for preparing the glass ceramics. The glass-ceramics were prepared by melting the mixture, quenching into water, and then annealed at various temperatures. The details are described as following.

Each batch, 1000 g, was mixed thoroughly by ball milling. The mixture was put into an alumina crucible and melted at 1500 ºC for 1 h in air in a furnace. The melts was poured into cold water to obtain the basic glass particles that have the black shining appearance.

The DSC-TG analysis was carried out by using a DSC-TG analyzer (SDTQ600, USA) to valuate the crystallization properties of the basic glass, and also to analyze the related glass-transition temperature, nucleation temperature, crystallization and/or phase transition temperature. Measurements were performed by heating the basic glass powders from 20 ºC to 1200 ºC in air, and the pure Al_2O_3 was used as the reference material. The basic glass particles were ground into granules, and then put into alumina crucibles for the different annealing/sintering heat treatments according to the differential scanning calorimeter and thermo gravimetric (DSC-TG) analysis. The temperatures for the heat treatments are 700 ºC, 900 ºC, 1100 ºC, 1135 ºC, and 1200 ºC, respectively.

Porous glass-ceramics were prepared by mixing 85% of basic glass powders and 15% of foaming agent Na_2CO_3, pressing into green pellets with 50 mm in diameter and about 20 mm in thickness, sintering at 840 ºC for 120 min.

Phase component and microstructures of the glass-ceramics heat-treated at various temperatures were investigated by using X-ray diffraction (XRD, Rigaku D/Max-2500 diffractometer with Cu K_α radiation) and scanning electron microscope (SEM, FEI Quanta-200), respectively. The glass-ceramics were ground, polished and etched in HF solution (5%) for 60 s, and were sprayed platinum onto the surface to improve the conductivity for SEM observations. Magnetic hysteresis loops were recorded by a Lakeshore vibrating sample magnetometer (VSM) in to applied fields of ±10 kOe, at ambient temperature. The hardness of the prepared glass-ceramics was tested by using HVA-10A Vickers micro-hardness measurement system at a load of 1000 g. For the thermal conductivity investigation, the samples were cut into wafers with diameter of 10 mm, thickness of 5 mm. Thermal diffusivities were measured by using a JR-2 thermophysical properties tester at room temperature.

3 Results and discussion

3.1 DSC-TG analysis

Figure 1 shows the DSC-TG curves of the basic glass powder. It can be seen that the glass transition temperature (T_g) is around 589.2 ºC, at which the first exothermic peak appeared. At 680 ºC, a small endothermic peak exists. The peak from the thermal effect might be caused by the molecular rearrangement in glass, indicating that the crystalline nuclei may form around 680 ºC. To accelerate the particle migration, the nucleation temperature should be higher than 680 ºC, so that the nucleation temperature was selected as 700 ºC in the present work. Subsequently, three exothermic peaks appear at 706.7 ºC, 895.9 ºC and 1096.1 ºC, respectively. Meanwhile, from the TG curve, the sample mass increased at 706.7 ºC, and decreased slightly at 895.9 ºC and 1096.1 ºC.

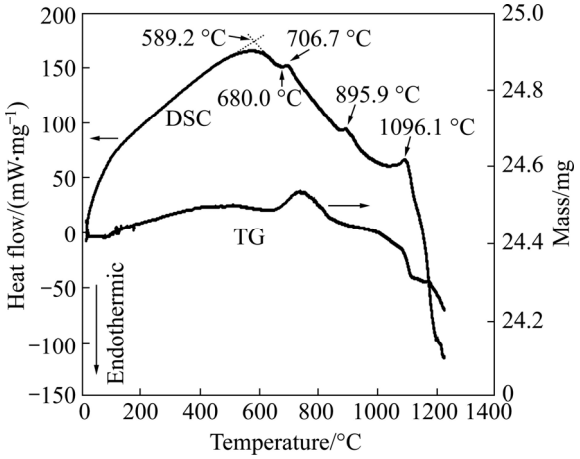

Fig. 1 DSC-TG curves of basic glass

From the DSC-TG curves, one can get the clues that oxidation of metal ions such as like Fe^{2+} ions might take place and some phases with low melting point might produced around 706.7 ºC, and phase formation and/or phase transformation might occur around 895.9 ºC and 1096.1 ºC. While, the obvious mass loss and endothermic process take place at temperatures higher than 1096.1 ºC, indicating that the crystallized glass-ceramic starts to re-melt again. At the temperature higher than 706.7 ºC, the sample shows mass-loss process, it should be resulted from the volatilization of some low-melt point phases.

3.2 XRD phase investigation

The XRD patterns of the samples heat-treated at various temperatures are shown in Fig. 2. Figure 2(a) shows a XRD pattern of the basic glass heat-treated at 700 ºC for 3 h. Only some weak diffraction peaks can be seen, which illustrates that the crystallization degree is very low and the sample still keeps a glass characteristic. There are four kinds of possible phases existing in the treated glass. 1) The first one belongs to the space group of *Imma*, its crystal structure is the same as the olivine-type $Fe_{2.45}Si_{0.55}O_4$ (a=0.5866 nm, b=1.1885 nm and c=0.8338 nm). 2) The second one belongs to the space group of $C\bar{1}(2)$, and has the crystal structure as the same as sunstone-type (Ca, Na)(Al, Si)$_2$Si$_2$O$_8$ phase (a=0.8241 nm, b=1.2859 nm and c=0.7097 nm). 3) The third phase belongs to the space group of $P3_112$, whose crystal structure is in accord with the amblygonite-type $AlPO_4$ phase (a=b=0.4942 nm, c=1.0970 nm). 4) The crystal structure of the forth phase follows the amblygonite-type Al_3BO_6 phase (a=0.9510 nm，b=0.8110 nm and c=0.4290 nm).

According to the DSC-TG analysis as shown in Fig. 1, the heat-treatment temperature of 700 ºC is close to the nucleation temperature of the glass, and some crystal nucleuses may be formed. Fe element may exist in different phases in forms of Fe^{2+} and Fe^{3+}. So the olivine-type $Fe_{2.45}Si_{0.55}O_4$ phase should be the solid solution of Fe_3O_4-Fe_2SiO_4 [17]. Both B_2O_3 and P_2O_5 are glass network formers that are similar to SiO_2. Cations attracting for oxygen ions lead to the liquid phase separation in the oxide melt. The higher the field intensity of the cation is, the easier the oxygen ion is attracted. Because the field intensity of a P^{5+} ion is higher than that of a Si^{4+} ion, the P^{5+} ions can accelerate the composition regionalization and segregation in the silicate glass. Thereby, it can prompt the occurrence of crystal nucleus in the P^{5+}-rich regions. B_2O_3 glass is composed by boron oxygen group as [BO_3] and may transform to the type of [BO_4] when alkali-metal ions were introduced, resulting in the transformation of three dimensional framework structure. To strengthen the network, the crystal phases such as $AlPO_4$ and Al_3BO_6 containing P^{5+} and B^{3+} ions may form easily.

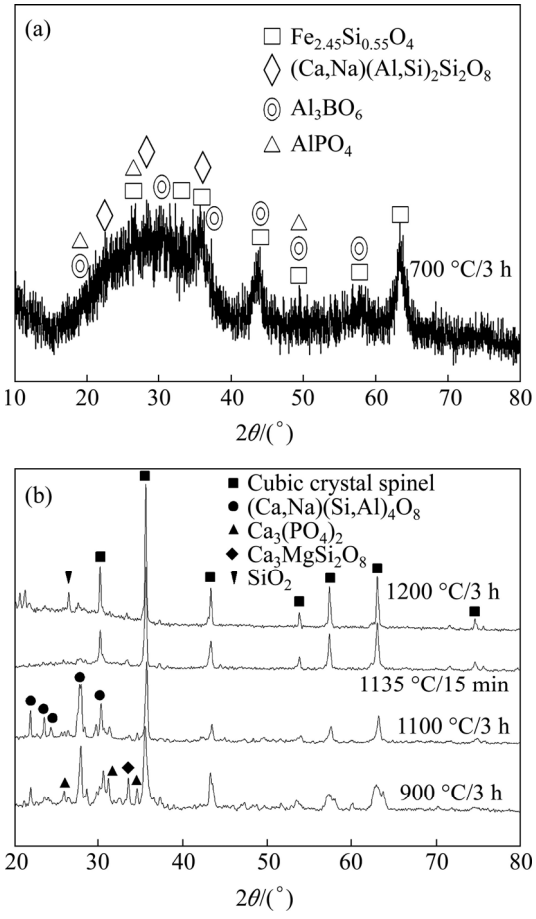

Fig. 2 XRD patterns of glass ceramics annealed at various temperatures: (a) 700 ºC; (b) 900 ºC, 1100 ºC, 1135 ºC and 1200 ºC

After the glass was heat-treated at 900 ºC, as shown in Fig. 2(b), the amount of the crystalline phases increased obviously, compared with the one heat-treated at 700 ºC. Two kinds of crystal phases can be detected obviously. One of them is a cubic spinel-type phase with the space group of $Fd\bar{3}m$ cited by the PDF number of 03-0864 (as denoted by "■"in Fig. 2(b)), and another is the sodium-calcium feldspar-type phase, (Ca, Na) (Si, Al)$_4$O$_8$ with the space group of $C\bar{1}(2)$ cited by the PDF number of 18-1202 (denoted by "▼"). At the same time, few small diffraction peaks can also be detected according to the compounds of $Ca_3(PO_4)_2$ and $Ca_3MgSi_2O_8$, which are referred to the PDF numbers of 09−0348 and 35−0591, respectively. The diffraction peaks of cubic system are strong, indicating that a part of the cubic-type crystal had separated out and ever grown up. While, $AlPO_4$ and Al_3BO_6 types of phases as detected in the sample treated at 700 ºC disappeared, and (Ca, Na)(Si, Al)$_4$O$_8$-type phase appeared. During the 900 ºC heat-treatment, the elements Al, P and B can dissolve into the aluminosilicate compounds such as sodium-calcium feldspar as detected in Fig. 2(a), and replaced Si and occupied the crystal lattice sites. When enough Al occupied the Si-sites in the sunstone-type crystal phase such as (Ca, Na)(Al, Si)$_2$Si$_2$O$_8$, the crystal phase transformed into the (Ca, Na)(Si, Al)$_4$O$_8$ type phase.

When the glass was heat-treated at 1100 ºC, the cubic spinel-type phase (reference phase is $NiFe_2O_4$ and referred to the PDF number of 86−2267) and the sodium-calcium feldspar-type (Ca, Na)(Si, Al)$_4$O$_8$ phase (denoted by "●"in Fig. 2(b)) are still the main crystal phases. It is notable that the diffraction peaks become more sharpened compared with the ones of 900 ºC. The cubic crystal further grew up and new cubic system crystal separated out probably. Meanwhile, the diffraction peaks

coming from the phases like $Ca_3MgSi_2O_8$-type and $Ca_3(PO_4)$- types crystals disappeared after the sample was heated at 1100 °C. They transformed into the sodium-calcium feldspar-type phase because of the diffusion and solid solution of those elements. According to thermodynamic calculation and structural properties for the FeO-SiO_2 system [18], the melting temperature of Fe_2SiO_4 is (1177±20) ºC. Thus, the cubic system Fe_2SiO_4 may be in the state of fusion at 1100 ºC, being favorable to the diffusion and migration of the relative elements. Additionally, the Fe^{2+} ions in the glass-ceramics may be oxidized to Fe^{3+} ions gradually with the increase of temperature. On the other hand, the Fe^{3+} ions and other elements (such as Ni, Co, Mn, Mg, etc) will form the cubic ferrite spinel-type phase that is similar to the one of $NiFe_2O_4$ as detected in this XRD pattern.

As shown in Fig. 1, the mass loss of the glass-ceramics took place at temperatures higher than 1096.1 ºC. According to the XRD pattern as shown in Fig. 2(b), after the sample was heat-treated at 1200 ºC, the content of the glass phase increased, and a few SiO_2 phase and other new impurity phases formed compared with the ones treated at 1100 ºC. And the cubic spinel-type crystalline grain grew up further, as indicated by the more sharpened diffraction peaks of cubic phase. At the same time, re-melt of some crystals happened because of the high temperature.

When the basic glass was heat-treated at 1135 ºC for 15 min following the nucleating treatment at 700 ºC, the glass ceramic has the cubic spinel-type phase that is in accordance with the crystal structures of Fe_3O_4 and $NiFe_2O_4$, which are referred to the PDF numbers of 75−6449 and 86−2267, respectively. The XRD pattern is shown in Fig. 2(b). The other crystalline phases as shown in the glass ceramics heat treated at the temperatures lower than 1135 ºC can not be detected in the XRD pattern, and should be melted or transformed into the amorphous phase again.

Please note that, all the glass-ceramics obtained by heat-treatment at 900, 1100 or 1135 ºC show the black shining appearance. The microstructure evolution was investigated by SEM observations as displayed in the next section.

3.3 SEM investigation

Figure 3 shows the SEM observations of the glass-ceramics heat-treated at 900, 1100 and 1200 ºC, respectively. When the sample was heat-treated at 900 ºC, it is mainly composed of glass phase, and a few white-color particles distributing in the glass can be observed (as shown in Fig. 3(a)). Compared with Fig. 2(b), the white particles should belong to the cubic spinel-type

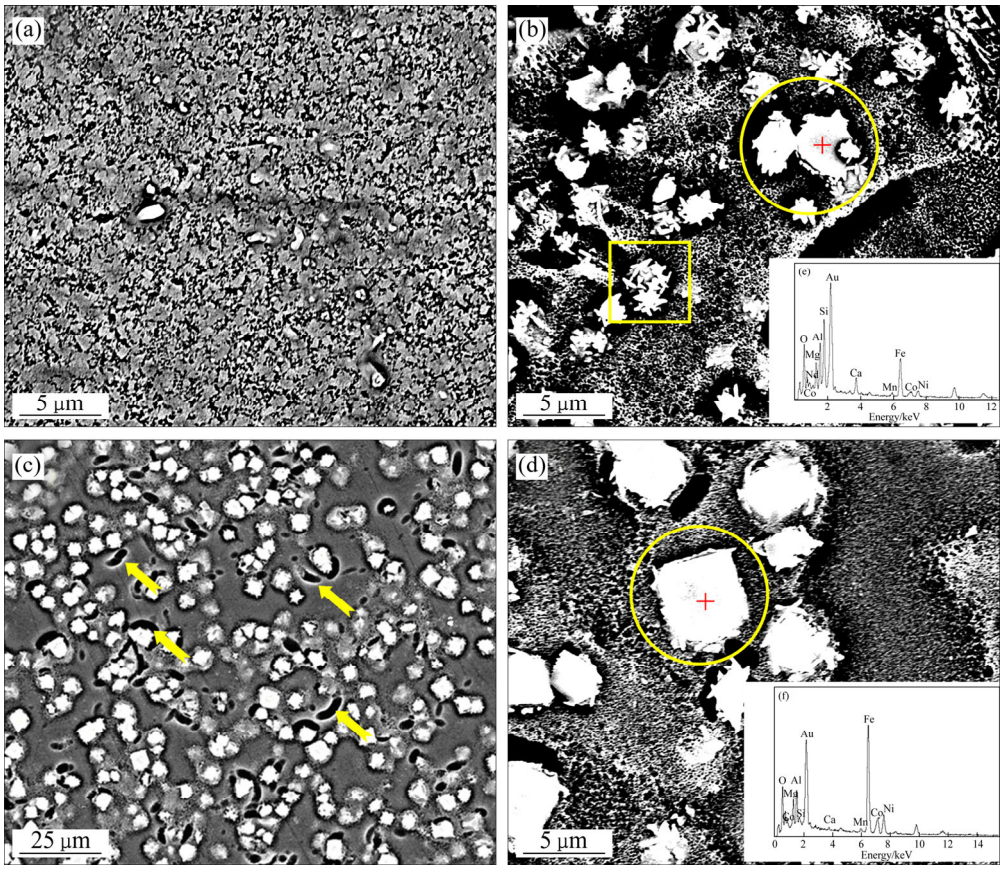

Fig. 3 SEM investigations of glass ceramics heat-treated at various temperatures: (a) 900 °C, (b) 1100 °C; (c), (d) 1200 °C; (e) EDS pattern in Fig. 3(b); (f) EDS pattern in Fig. 3(d)

crystal phase. These crystalline grains are less than 1 μm.

After heat treatment at 1100 ºC, as seen in Fig. 3(b), the amount of crystal phases increased and the crystalline particles grew up. There are two kinds of morphologies of the crystalline phases, spear-like one (as marked with a square) and gooseberry-like one (as marked with a circle in Fig. 3(b)). Figure 3(e) shows an energy disperse spectroscopy (EDS) recorded from the white-color particles as marked by a cross "+" inside the circle in Fig. 3(b). The Au EDS peak results from the sprayed gold in order to improve the conductivity for SEM observation. According to XRD analysis in Fig. 2(b), the gooseberry-like grains should be the cubic spinel-type phases. The cubic spinel-type phases could be the ferrite phases with the molecular formula like AB_2O_4, where, A-site can be Fe, Ni, Co, Mn and/or Mg, and B-site can be Fe, Al, etc. The spear-like phase should be the sodium-calcium feldspar-type phase such as $(Ca, Na)(Si, Al)_4O_8$ detected in Fig. 2(b). Additionally, olivine-type $Fe_{2.45}Si_{0.55}O_4$ phase maybe still remained in the particles according the remained content of Si in the EDS diagrams.

Figures 3(c) and (d) show the SEM observations of the glass-ceramics heat-treated at 1200 ºC. It is obvious that the cubic spinel-type crystals grew up further, comparing with that heat-treated at 1100 ºC, and the grain size approaches to 5 μm. A great amount of black worm shape grooves shown in Fig. 3(c) (some of them are noted by arrows), demonstrating the re-melt phenomenon of the glass ceramics. This is in accordance with the declining TG curve as shown in Fig. 1. Figure 3(f) shows an EDS recorded from the white particles marked by "+" inside the circle in Fig. 3(d). Compared with Fig. 3(e), the contents of Co, Ni and Fe increased while the contents of Si and Al decreased obviously. Combining with the XRD analysis in Fig. 2, the phase could be spinal ferrite with an AB_2O_4 type such as MFe_2O_4 (M=Fe, Ni, Co, Mg). These kinds of compounds always show magnetic property.

3.4 Magnetic properties

The magnetic hysteresis loops were recorded by a Lakeshore vibrating sample magnetometer in present work. Figure 4 shows the magnetic hysteresis loops of the glass-ceramics heat-treated at different temperatures. The saturation magnetizations (M_s) are 0.6778, 1.4243, 2.9055 and 2.9557 emu/g after the basic glass was heat-treated at 700, 900, 1100 and 1200 ºC, respectively. The magnetic property of the sample heat-treated at 700 ºC is very weak and negligible, and the magnetism of the glass-ceramics becomes obvious when the heat-treatment temperatures are above 900 ºC. The M_s increases with the treatment temperature increasing. According to the XRD analysis in Fig. 2 and the SEM investigations in Fig. 3, the cubic spinel-type phases occurred and their amount as well as the size of the related crystalline particles increased with the heat-treatment temperature increased. The obvious growth of crystal particles and the quantities increasing of crystalline phases, especially, of the cubic spinel phase were observed when the heat-treatment was carried out at higher temperatures such as from 900 ºC to 1100 ºC.

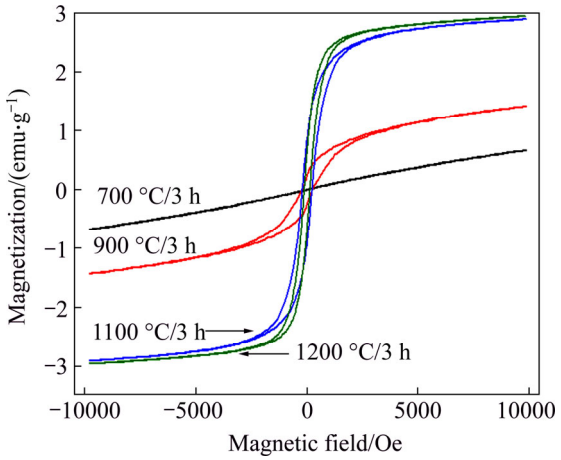

Fig. 4 Magnetic hysteresis loops of glass ceramics annealed at various temperatures

As discussed above, the cubic spinel-type phases possibly belong to and or contain the ferrite that always displays a magnetic property. These indicate that the cubic spinel phases act as the important contribution to the magnetic property.

3.5 Porous glass-ceramic and thermal conductivity

Figure 5 shows the SEM observations of the porous glass ceramic made from the iron-tailing glass (PGC1) with 15% Na_2CO_3 (mass fraction) as the foaming agent. One can see that the porous glass ceramic has a nearly homogeneous microstructure (see in Fig. 5(a)) and the pore sizes range about 2−5 μm (see in Fig. 5(b)). The density is measured to be 1.39 g/cm^3, and the porosity is calculated to be 47.3% compared with the density of the dense glass ceramic (2.64 g/cm^3). As shown in Fig. 6, a cubic spinel-type phase matching with Fe_3O_4 (referred to the PDF number of 79-0416), which can be re-written as $FeFe_2O_4$ and always has a magnetic property, in the porous glass ceramic can be indexed in the XRD pattern.

The thermal conductivity (λ) of the porous glass ceramic made from iron tailings (PGC1) was tested. For comparison, the thermal conductivities of a dense glass ceramic (DGC) made from the iron tailings and a porous glass ceramic made by using commercial glass (PGC2) were also tested. The PGC2 was prepared at the same condition as that of PGC1. The densities of the PGC1, PGC2 and DGC were measured as 1.39, 1.07 and 2.64 g/cm^3, respectively. The λ of PGC1

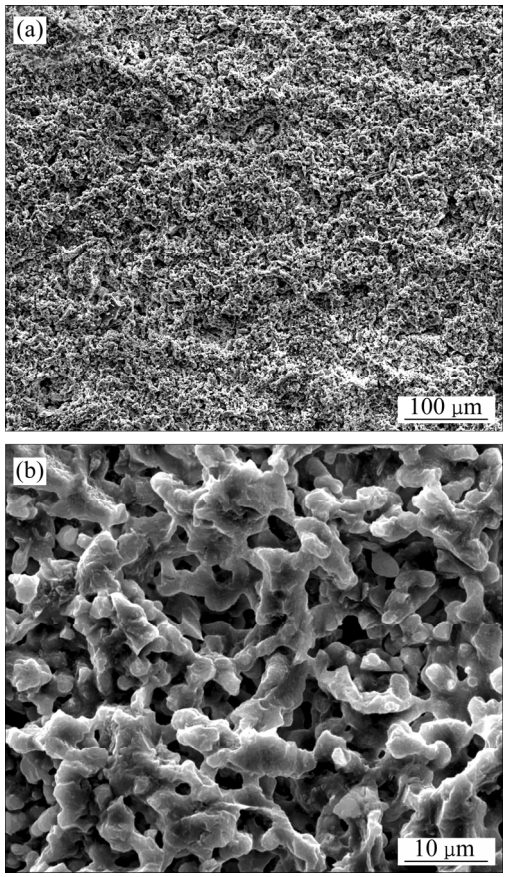

Fig. 5 SEM observations of porous glass ceramic made from iron tailings: (a) Low magnification; (b) High magnification

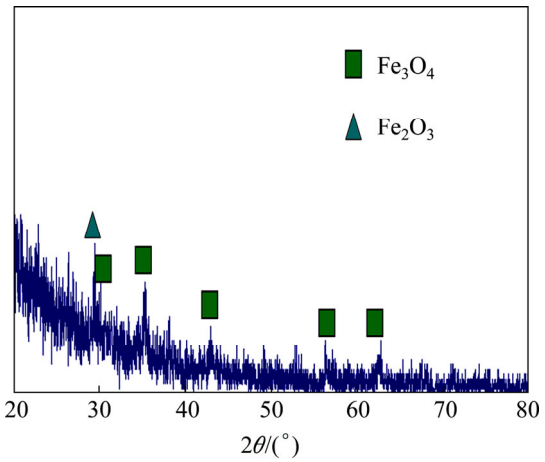

Fig. 6 XRD pattern of porous glass ceramic made from iron tailings

(0.361 W/(m·K)) is the smallest one. The λ of PG1 is about one fifth of the one of DGC (1.848 W/(m·K)), and is about 56% of the one of PGC2 (0.642 W/(m·K)). Although the density of PGC1 is higher than that of PGC2, the PGC1 has a much lower thermal conductivity. These indicate that the porous glass ceramic made from iron tailings has good thermal insulation.

It is well known that there generally are three types of thermal transports in a solid state matter: 1) thermal convection taking place by the gas flow and gas molecular collision; 2) thermal conduction depending on the reaction among the phonons and free electrons, and 3) thermal radiation for the electromagnetic radiation (i.e., photon movement) that always occurs at elevated temperatures and is very weak at ambient temperatures.

In the present work, because the thermal conductivities of all the samples were measured at room temperature, the thermal radiation should be negligible. Since the electrical resistivities of the three samples are greater than 10^9 Ω/cm at room temperature, the free electrons contribute hardly any effect in the thermal conduction. Therefore, the thermal transport is closely related to the gas status and microstructure characteristic such as phonons, magnetic elements and crystal interfaces in the present work. The gas inside the porous samples can be considered to be stationary and has the λ of about 0.024 W/(m·K), which is much lower than those of the inorganic materials [3]. One can get that the thermal conductivities of porous glass ceramics are lower than that of the dense ceramic, as shown in the present work. On the other hand, the difference of the thermal conductivities between PGC1 and PGC2 should result from the influencing factor on the transport process of the phonons. As discussed above, the glass ceramics made from the iron ore tailings consist of the phases with magnetic characteristic. The spin-phonon interaction and the phonons scatting induced by the magnetic elements may result in that the λ of the phonons is suppressed [19−20]. Therefore, for the porosity and the existence of magnetic component, the thermal conductivity of the porous glass ceramic made from iron tailings is lower than that of the dense glass ceramic made from the iron tailings, and is even lower than that of the porous glass ceramic made by using commercial glass.

4 Conclusions

1) The magnetic glass-ceramics are prepared by using iron ore tailings as the main raw materials.

2) Orthorhombic olivine-type phase and triclinic sunstone-type phase form when the basic glass is annealed at 700 ºC. The concentration of olivine-type and sunstone-type phases decreases, the cubic spinel-type phases occur and their amounts increase, when the annealing temperature increases. The cubic spinel-type ferrite phases become the main crystals in the glass-ceramics after the basic glass is annealed at temperatures higher than 1100 ºC.

3) The prepared glass-ceramics have a magnetic property which closely depends on the heat-treatment temperature. The magnetism is proposed to result from the formation of the cubic spinel-type ferrite phases.

4) The thermal conductivity of the porous magnetic

glass ceramic is much lower than that of the dense glass-ceramics, and is even lower than that of the non-magnetic porous glass ceramic without magnetism.

References

[1] SUN Hong-fei, LI Yong-hua, JI Yan-fang, YANG Lin-sheng, WANG Wu-yi, LI Hai-rong. Environmental contamination and health hazard of lead and cadmium around Chatian mercury mining deposit in western Hunan Province, China [J]. Transactions of Nonferrous Metals Society of China, 2010, 20: 308−314.

[2] DAS B, PRAKASH S, REDDY PSR, MISRA VN. An overview of utilization of slag and sludge from steel industries [J]. Resources, Conservation and Recycling 2007, 50: 40−57.

[3] LUIZ H, MACCARINI V, JAUME A. Recycling concepts and the index of recyclability for building materials [J]. Resources, Conservation and Recycling, 2013, 72: 127−135.

[4] SAKTHIVEL R, VASUMATHI N, SAHU D, MISGRA B K. Synthesis of magnetite powder from iron ore tailings [J]. Powder Technology, 2010, 201: 187−190.

[5] WANG X L, REN R C, LIU Y. Application of DTA in preparation of glass-ceramic made by iron tailings [J]. Procedia Earth and Planetary Science, 2009, 1: 750−753.

[6] WATSON J H P, BEHARRELL P A. Extracting values from mine dumps and tailings [J]. Minerals Engineering, 2006, 19: 1580−1587.

[7] BERNARDO E, EDME E, MICHON U, PLANTY N. Fast-sintered gehlenite glass-ceramics from plasma-vitrified municipal solid waste incinerator fly ashes [J]. Journal of the American Ceramic Society, 2009, 92: 528−530.

[8] EROL M, KÜCÜKBAYRAK S, ERSOY-MERICBOYU A. Comparison of the properties of glass, glass-ceramic and ceramic materials produced from coal fly ash [J]. Journal of Hazardous Materials 2008, 153: 418−425.

[9] LUAN J, LI A, SU T, CUI X. Synthesis of nucleated glass-ceramics using oil shale fly ash [J]. Journal of Hazardous Materials, 2010, 173: 427−432.

[10] ZHAO T, LI B W, GAO Z Y, CHANG D Q. The utilization of rare earth tailing for the production of glass-ceramics [J]. Materials Science and Engineering B, 2010, 170: 22−25.

[11] YU Hong-hao, XUE Xiang-xin, HUANG Da-wei. Crystallization on BaO-Fe_2O_3-SiO_2 glass-ceramic made from iron ore tailing [J]. The Chinese Journal of Nonferrous Metals, 2008, 18(11): 2076−2081. (in Chinese)

[12] LI Bao-wei, DU Yong-sheng, ZHANG Xue-feng, JIA Xiao-lin, CHEN Hua, ZHAO Ming, DENG Lei-bo. Influence of basic composition ratio on structure and properties of slag glass-ceramics prepared by baiyunebo tailing [J]. Journal of Synthetic Crystals, 2012, 41(5): 1391−1398. (in Chinese)

[13] SUN Xiao-hua, WANG Ming-pu, LIN Dian-liang, XIONG Yong-jun. A new type of tungsten tailings glass-ceramics [J]. Journal of Central South University (Science and Technology), 1997, 28(5): 448−451. (in Chinese)

[14] SHI Pei-yang, ZHANG Yi, ZHANG Da-yong, WANG Yuan-yuan, JIANG Mao-fa. Crystallization behavior and properties of glass ceramic of ferrous tailings and slag [J]. The Chinese Journal of Nonferrous Metals 2007, 17(2): 341−347. (in Chinese)

[15] GAO Jie, XU Chang-wei, ZHANG Yang, YANG Meng-hui. The Influence of compositions of raw materials on the physical properties of porous glass-ceramics based on iron tailings [J]. Bulletin of the Chinese Ceramic Society, 2012, 31(6): 1417−1420. (in Chinese)

[16] Huang S X, Ding L, Deng L W. Production and properties of cordierite-based glass-ceramics from gold tailings [J]. Materials Science and Engineering of Powder Metallurgy, 2011, 16: 553−556. (in Chinese)

[17] WOODLAND A B, ANGEL R J. Crystal structure of a new spinelloid with the wadsleyite structure in the system Fe_2SiO_4-Fe_3O_4 and implications for the Earth's mantle [J]. American Mineralogist, 1998, 83: 404−408.

[18] SEO W G, TSUKIHASHI F. Thermodynamic and structural properties for the FeO-SiO_2 system by using molecular dynamics calculation [J]. Materials Transactions, 2005, 46: 1240−1247.

[19] SLACK GA. Thermal conductivity of CaF2, MnF_2, CoF_2 and ZnF_2 Crystals [J]. Physical Review, 1961, 122: 1451−1464.

[20] SLACK GA, NEWNAN R. Thermal conductivity of MnO and NiO [J]. Physical Review Letters, 1958, 1: 359−360.

(Edited by HE Yun-bin)